

1 **Integration of geophysical and groundwater electrical conductivity data**
2 **in a coastal aquifer for monitoring saltwater intrusion dynamics**

3 Lorenzo De Carlo¹, Maria Clementina Caputo¹, Rita Masciale¹, Antonietta
4 Celeste Turturro¹, Ivan Portoghese¹, Giuseppe Passarella¹

5 ¹ National Research Council of Italy – Water Research Institute, Via F. De
6 Blasio 5 70132 Bari, Italy
7 lorenzo.decarlo@cnr.it

8 **Abstract.**

9
10 This research focuses on monitoring saltwater intrusion dynam-
11 ics in a coastal aquifer in Southern Italy.

12 In the Torre Guaceto area, a multidisciplinary approach, based
13 on the geophysical Electromagnetic Induction (EMI) technique
14 and groundwater electrical conductivity (EC) data was applied.
15 The EMI survey was carried out, between November 2022 and
16 January 2024, along a 2.5 km transect, perpendicular to the coast-
17 line covering both agricultural and wetland landscapes. The data
18 were collected over time to assess the space-time variation of the
19 bulk EC. Likewise, the groundwater's EC was monitored using
20 probes installed in two wells and a coastal pond at varying dis-
21 tances from the sea along the transect. The geophysical model
22 helped identify a highly conductive plume potentially associated
23 with saltwater intrusion, determine the plume's extent, and moni-
24 tor coastal dynamics by tracking its evolution over time. The con-
25 tinuous EC groundwater values recorded at the monitoring points,
26 situated at increasing distances from the coastline, confirmed the
27 findings of the geophysical model. This integrated approach has
28 proven reliable for monitoring saltwater intrusion dynamics in
29 coastal aquifers at different spatial scales.

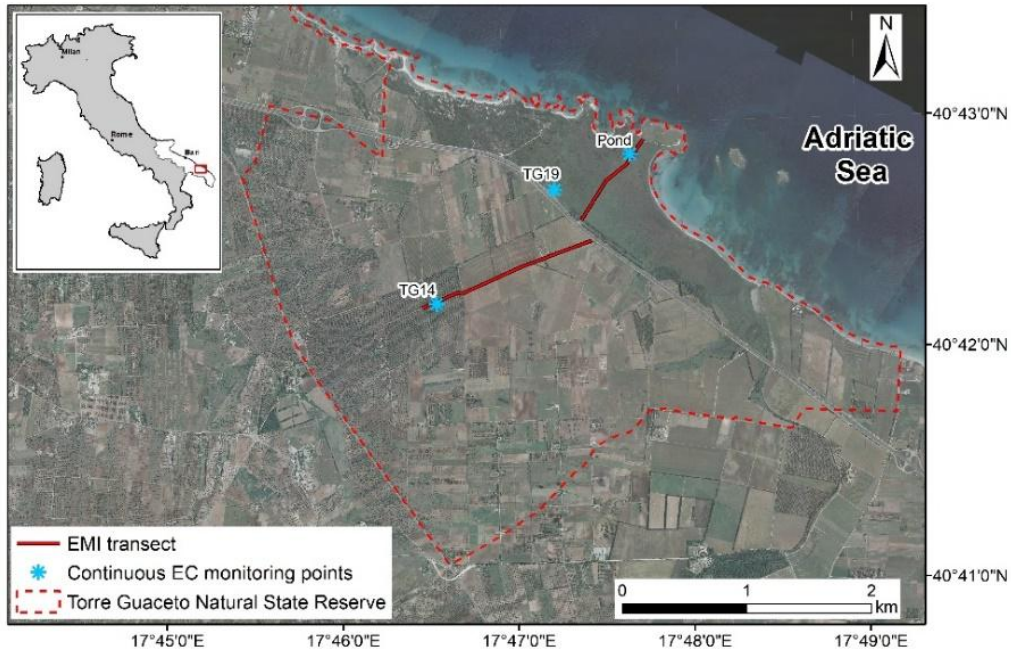
30 **Keywords:** coastal aquifer dynamics, saltwater intrusion, inte-
31 grated monitoring, Electromagnetic Induction data, groundwater
32 electrical conductivity.

33 1 Introduction

34 The saltwater intrusion process strongly affects groundwater quality in Med-
 35 iterranean coastal areas, significantly reducing fresh water for drinking and ir-
 36 rigation over time.

37 In the past decade, an integrated approach based on geophysical techniques
 38 combined with traditional measurements in wells has been successfully em-
 39 ployed to investigate coastal aquifer dynamics. In particular, noninvasive geo-
 40 physical methods have been widely used due to their ability to detect soil mois-
 41 ture and salinity (De Carlo et al. 2024; McLachlan et al. 2021; von Hebel et al.,
 42 2014). Additionally, conventional hydrogeological measurements from wells
 43 are usually used to gain direct information about groundwater quality (Frollini
 44 et al., 2022; Hanafy & Benaafi, 2024).

45 This integrated approach was applied to the Torre Guaceto study area (Fig.1),
 46 a Natural State Reserve hosting a coastal wetland surrounded by an intensive
 47 agricultural landscape in the southeastern part of the Apulia region (Southern
 48 Italy). In its agricultural portion, this transect passes through rainfed crops (ol-
 49 ive groves and winter wheat) and irrigated vineyards supplied by saline ground-
 50 water wells. The approach aimed to define the area's hydrogeological charac-
 51 teristics, identify a highly conductive plume associated with saltwater intrusion,
 52 determine the extent of the plume, and monitor coastal dynamics by tracking
 53 the plume's evolution over time.

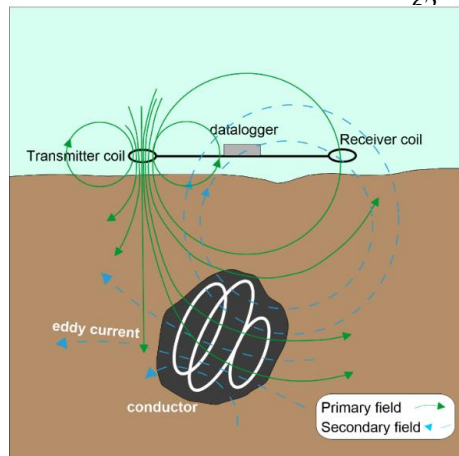


54
 55

Fig. 1. Location of the experimental site.

56 2 Materials and Methods

57 The electromagnetic Induction (EMI) technique, also called Frequency Do-
 58 main Electromagnetics (FDEM), is based on the induction of electrical currents
 59 in the conductive subsurface through electromagnetic waves generated on the
 60 surface. Fig. 2 shows a simple description of the basics. EMI measurements do
 61 not require any galvanic contact between the sensor and the conductive me-



76 **Fig. 2.** Basics of EMI technique

77
 78 The components of the secondary field that are in phase with the primary
 79 transmitted field and that portion that is 90 degrees out of phase (the quadrature
 80 component), are measured by a data logger. Under normal subsurface condi-
 81 tions, the in-phase component is strongly affected by buried metallic objects,
 82 while the quadrature component is directly related to the subsurface conductiv-
 83 ity (McNeill, 1980).

84 In the experimental site, the EMI campaigns were performed between No-
 85 vember 2022 and June 2024 along the same transect 2.5 Km long, located about
 86 perpendicular to the coastline (Fig. 1). The CMD DUO sensor (GF Instruments
 87 s.r.o., Czech Republic) collected electromagnetic data. The sensor consists of
 88 two independent coils, a transmitter, and a receiver connected by a flexible cab-
 89 ble. The transmitter coil is energized with an alternating current at 925 Hz, the
 90 receiver can be used at various inter-coil distances from the transmitter, one at
 91 a time. In this study, a combination of three different cables (10 m, 20 m, and
 92 40 m long) and coils configuration (VCP and HCP) was used to deepen the
 93 investigation to the maximum depth.

94 Since the data collected in the field are apparent electrical conductivity (ECa)
 95 they were processed through an inversion procedure to obtain an accurate dis-
 96 tribution of the true electrical conductivity. The EM4SOIL code (EMTOMO)
 97 uses a nonlinear smoothness-constrained inversion algorithm for producing

dium.
 In addition, EMI data are on-the-go
 field measurements, allowing the
 gathering of a large amount of spatial
 data in a relatively short time. A trans-
 mitter coil generates an alternate cur-
 rent that spreads into the subsurface.
 As the electromagnetic (EM) waves
 travel through different materials,
 eddy currents induce secondary EM
 fields. At the surface, a receiver coil
 records a signal that is the sum of the
 primary and secondary fields.

98 quasi-2D conductivity imaging. A forward modeling subroutine, based on the
99 cumulative function, is used for solving the EM fields and calculating the the-
100 oretical ECa responses at the nodes of a tridimensional mesh of hexahedral
101 blocks, distributed according to the locations of the measurement points.

102 The data were collected at three different time points to evaluate the changes
103 in electrical conductivity over time. Along such transect, the EC of the ground-
104 water was monitored using a submersible data logger for long-term monitoring
105 (CTD-Diver®, Van Essen Instruments B.V.) installed at different distances
106 from the sea: in two wells (TG14, TG19) and the pond (PND00) (Fig. 1).

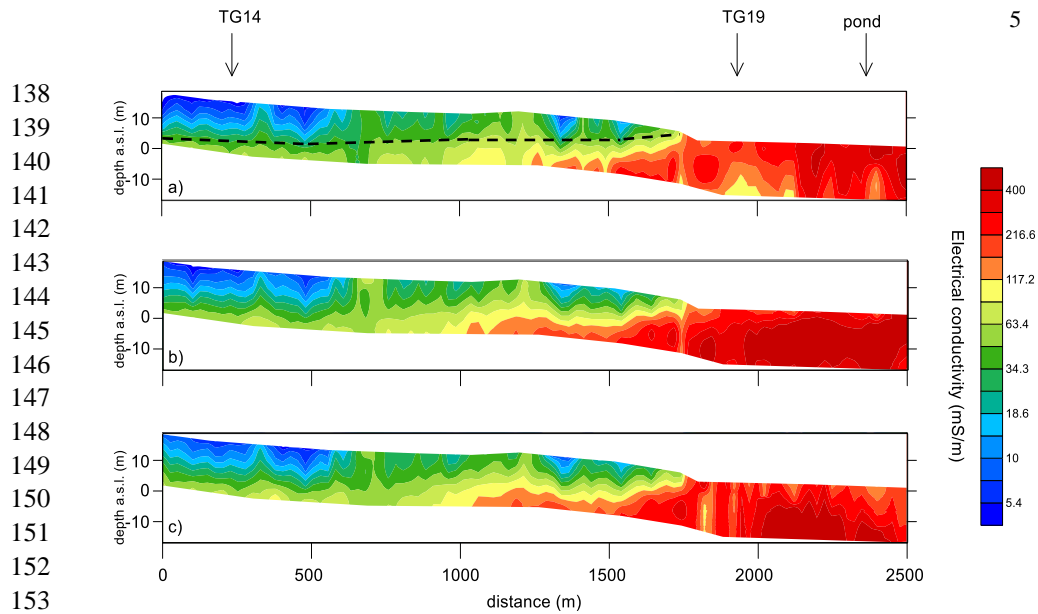
107 **3 Results and discussion**

108 Figure 3 shows the EMI cross-sections taken from November 2022 to Janu-
109 ary 2024. On November 22 (Figure 3a), a layered model was observed upstream
110 of the cross-section, consisting of an upper resistive body ($EC < 20$ mS/m)
111 overlaying a lower conductive layer ($20 < EC < 70$ mS/m) below the rein-fed
112 olive grove. A sloping discontinuity surface (black dotted line) marks the tran-
113 sition between the resistive unsaturated zone and the conductive groundwater.
114 Moving downstream, the upper resistive layer thins and eventually disappears
115 at approximately 1800 m from the start of the cross-section. Meanwhile, the
116 electrical conductivity of the bottom layer increases as we move towards the
117 sea, about 1250 m from the start of the section, due to groundwater salinity
118 rising ($EC > 10$ mS/m up to 200 mS/m).

119 Approximately a year later, in September 2023, the highly conductive body,
120 associated with the salt wedge, intruded about 200-250 m inland (Figure 3b).
121 Moreover, significant variations in EC were observed in the area closest to the
122 sea. In particular, the EC increased by about 30% near the pond in September
123 2023 compared to November 2022. In January 2024, the trend observed in Sep-
124 tember 2023 was confirmed, indicating negligible movement of the salt wedge
125 (Figure 3c). Meanwhile, the EC in the area towards the sea had returned to lev-
126 els comparable to November 2022. In addition, on top of the profile, the alter-
127 nation between higher and lower resistive bodies is preserved thus underlining
128 a possible correlation between saline water irrigation and the 2D patterns of EC
129 in the unsaturated zone.

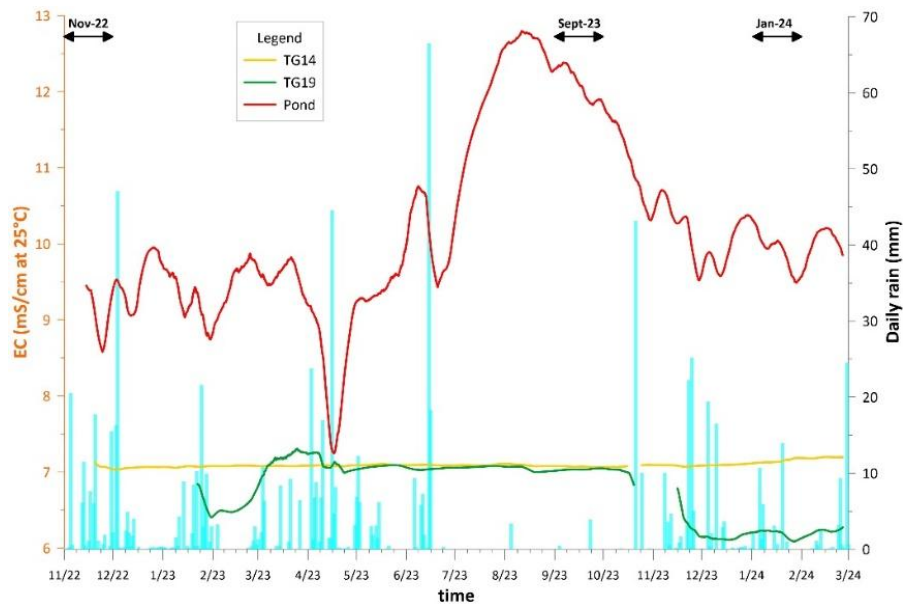
130 Direct EC measurements in groundwater along the transect closely reflect
131 the trend identified by geophysical techniques (Figure 4) showing a progressive
132 salinity influence from inland to the coast.

133 The EC values in well TG14 remain almost constant throughout the moni-
134 toring period, well TG19 shows a consistent EC increase during the irrigation
135 period, while the EC measured in the pond is extremely variable in time being
136 affected by precipitation during the Winter (decrease) and withdrawals and
137 evaporation phenomena during the Summer (increase).



154 **Fig. 3.** Inverted EMI cross-sections referred to: a) November 2022; b) Sep-
155 tember 2023; c) January 2024

156



157

158 **Fig. 4.** Continuous monitoring of EC values (running average-window width 1
159 week) recorded in the monitoring points TG14, TG19 and pond. The periods of
160 geophysical surveys are also indicated.

161 **4 Conclusions**

162 The integrated approach has proven to be an effective tool for monitoring salt-
 163 water intrusion dynamics at various spatial scales. The comparison between di-
 164 rect EC measurements in groundwater and EMI outputs confirmed the latter's
 165 strong potential for revealing details about subsurface structures that would oth-
 166 erwise remain unpredictable without widespread point measurements. The
 167 adopted approach seems also promising for investigating salinization in the un-
 168 saturated zone caused by irrigation with saline waters.

169 **Funding**

170 This research was partially funded by the NextGenerationEU, within PRIN PNRR
 171 FU.CO.KA Project - Future scenarios in coastal karst: saltwater intrusion, loss of water
 172 resources and sinkhole development as effects of climate changes, P2022JZHKM.

173 **References**

- 174 1. De Carlo, L., Turturro, A.C., Caputo, M.C., Sapiano M., Mamo, J., Balzan,
 175 O., Galea, L., Schembri, M.: Mapping saltwater intrusion via Electromag-
 176 netic Induction (EMI) for planning a Managed Aquifer Recharge (MAR)
 177 facility in Maltese Island Acque Sotteranee - Italian Journal of Groundwa-
 178 ter 13(1), 07–15 (2024).
- 179 2. Frollini, E., Parrone, D., Ghergo, S., Masciale, R., Passarella, G., Pennisi,
 180 M., Salvadori, M., Preziosi, E.: An integrated approach for investigating the
 181 salinity evolution in a Mediterranean coastal karst aquifer. *Water* 14 (11),
 182 1725 (2022).
- 183 3. Hanafy, S., Benaafi, M.: Investigating seawater intrusion and salinization
 184 using the integration of hydrochemical and geoelectrical techniques. *Geo-*
 185 *physics* 89(5), B329-B338 (2024).
- 186 4. McLachlan, P., Blanchy, G., Chambers, J., Sorensen, J., Uhlemann, S., Wil-
 187 kinson, P., Binley, A.: The application of electromagnetic induction meth-
 188 ods to reveal the hydrogeological structure of a riparian wetland. *Water Re-*
 189 *sources Research*, 57(6) 1–20 (2021).
- 190 5. McNeill JD. Electromagnetic terrain conductivity measurement at low in-
 191 duction numbers: Geonics, Technical Note TN-6 (1980). Available at:
 192 <http://www.geonics.com/pdfs/technicalnotes/tn6.pdf>
- 193 6. von Hebel, C., Rudolph, S., Mester, A., Huisman, J.A., Kumbhar, P., Ve-
 194 reecken, H., van der Kruk, J.: Three-dimensional imaging of subsurface
 195 structural patterns using quantitative large scale multiconfiguration electro-
 196 magnetic induction data. *Water Resources Research* 50(3), 2732–2748
 197 (2014).